Systematic Investigation of Thorium(IV)– and Uranium(IV)–Ligand Bonding in Dithiophosphonate, Thioselenophosphinate, and Diselenophosphonate Complexes

Andrew C. Behrle,[†] Charles L. Barnes,[†] Nikolas Kaltsoyannis,*[,‡] and Justin R. Walensky*[,†]

[†]Department of Chemistry, University of Missouri−Columbia, 601 S. College Avenue, Columbia, Missouri 65211-7600, United States
[‡]Department of Chemistry, Christopher Ingold Laboratories, University College London, 20 Gordon Street, London WC1H 0AJ, United Kingdom

Ⓢ *Supporting Information*

ABSTRACT: Homoleptic soft-donor actinide complexes of the general form $An[E_2PROR']_4$ were synthesized from salt metathesis between $ThCl_4(DME)_2$ or $UI_4(1,4\text{-dioxane})_2$ and $M[E_2PROR']$, M = Na, K, to yield **2** (An = Th, E = S, R = 4-$MeOC_6H_4$, R' = Me), **3** (An = Th, E = S, R = 4-$MeOC_6H_4$, R' = ^tBu), **4** (An = U, E = S, R = 4-$MeOC_6H_4$, R' = Me), **5** (An = Th, E = Se, R = C_6H_5, R' = Me), and **6** (An = U, E = Se, R = C_6H_5, R' = Me). In addition thorium and uranium thioselenophosphinate complexes **7** and **8** were produced from the reaction of $ThCl_4(DME)_2$ and $UI_4(1,4\text{-dioxane})_2$ and $Na[SSePPh_2]$, respectively. All compounds were characterized using elemental analysis, ^{1}H and ^{31}P NMR, and IR spectroscopy, and the U(IV) compounds were also examined with UV−vis spectroscopy. The ^{77}Se NMR spectrum of **5** reveals the first reported resonance with a Th−Se bond. The solid-state structures of **2**, **5**, **7**, and **8** were determined by X-ray crystallography. The actinide−ligand bonding was examined using density functional theory calculations in conjunction with quantum theory of atoms-in-molecules analysis and shows slightly increased covalency in actinide−selenium bonds than actinide−sulfur.
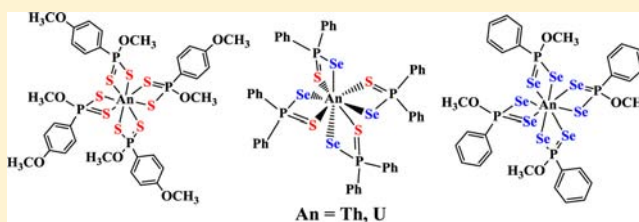
INTRODUCTION

The lanthanides and actinides share similar chemical properties such as high coordination numbers, Lewis acidity, decreasing ionic radius across each series with the lanthanide and actinide contractions, and oxophilic nature. One distinct difference between the two blocks is the increase in radial extension of the 5f orbitals, thus making covalent-type bonding accessible for 5f elements, while the 4f orbitals are contracted, affording limited orbital mixing and rendering bonding electrostatic in character. This could be an explanation for the selectivity that actinides show toward soft-donor ligands versus lanthanides[1−3] such as with dithiophosphinate, $[S_2PR_2]^-$, ligands.[4] As a result, actinide−ligand coordination chemistry and bonding with soft-donor ligands such as sulfur have received greater attention in recent years and lead to studies of minor actinide dithiophosphinate complexes of Am(III) and Cm(III) using X-ray absorption spectroscopy (XAS).[3,5,6] This also attracted our group to this area with the objective to create a series of homoleptic actinide complexes and make incremental changes in the coordination environment to examine how these affect actinide−ligand bonding.

While homoleptic tetravalent actinide complexes are well known, few with sulfur and selenium have been reported, Scheme 1. The earliest homoleptic thiolate complexes were synthesized by Gilman and co-workers from protonolysis of $U(NEt_2)_4$ with HSR, R = Et, ^nBu, in 1956.[7] Diethyldithio-carbamate complexes of thorium, uranium, neptunium, and plutonium were reported in 1967[8] and 1968[9] with the first crystal structures of homoleptic actinide complexes with all sulfur ligands being $Th(S_2CNEt_2)_4$[10] and $[Np(S_2CNEt_2)_4]^-$ in 1970.[11] Pinkerton and co-workers synthesized homoleptic dithiophosphinates, $[S_2PR_2]^-$, R = Me, Et, ^iPr, Ph, Cy, and dithiophosphates, $[S_2P(OR)_2]^-$, R = Et, ^iPr, of thorium with $Th(S_2PMe_2)_4$ and $Th(S_2PCy_2)_4$ being structurally elucidated.[12] In 1990, Gilje reported the first homoleptic uranium dithiolene complex, $Li_4(dme)_4U(edt)_4$.[13] It was not until the mid 1990s that Ephritikhine and co-workers started their work on uranium thiolate complexes of the form $[U(SR)_6]^{2-}$, R = Ph, ^iPr, ^tBu, ^nBu,[14,15] and expanded to homoleptic dithiolene uranium(III) and uranium(IV) complexes.[16,17] Bulky thiolate groups such as 2,4,6-tri-*tert*-butyl-thiolate (Mes*) have produced rare neutral U(IV) and U(III) complexes.[18] Further, a uranium(IV) compound coordinated with three $(SPS^{Me})^-$, SPS^{Me} = 1-methyl-2,6-bis(diphenylphosphine sulfide)-3,5-diphenylphos-phinine anion, ligands and an outer sphere iodide was also reported by Ephritikhine.[19] While not considered homoleptic, we also note that neutral compounds of uranium, U-$(EPh)_4(py)_3$, have also been made from uranium metal and PhEEPh (E = S, Se) with a catalytic amount of iodine in pyridine.[20]

Scheme 1. Known Homoleptic Tetravalent Actinide Complexes with Sulfur- and Selenium-Donor Ligands

[U(SPS)₃]I

[U(edt)₄]⁴⁻
[U(dddt)₃]²⁻
edt = ethane-1,2-dithiolate
dddt = 5,6-dihydro-1,4-dithiine-2,3-dithiolate

[U(SR)₆]²⁻
R = Ph, ⁱPr, ᵗBu, ⁿBu

U(Mes*)₄

An[S₂PR₂]₄
An = Th, Am, Cm
R = Me, Et, ⁱPr, Ph, Cy, OEt, OⁱPr, 2,4,4-
trimethylpentyl, n-octyl

An[Se₂PPh₂]₄
An = U, Np

An[S₂CNR₂]₄
An = Th, U, Np, Pu
R = Et, Cy
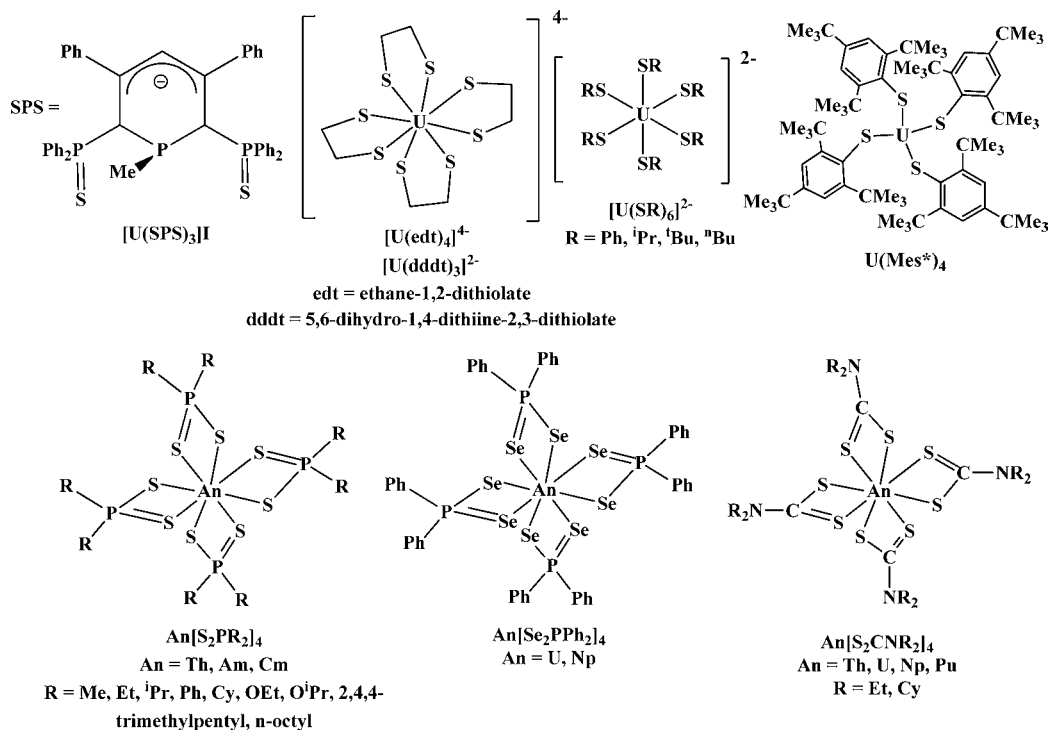
Table 1. X-ray Crystallographic Data Are Shown for Complexes 2, 5, 7, and 8

	2	5	7	8
CCDC deposit no.	933917	947438	933915	933916
empirical formula	$C_{32}H_{40}O_8P_4S_8Th$	$C_{28}H_{32}O_4P_4Se_8Th$	$C_{52}H_{48}OP_4S_4Se_4Th$	$C_{52}H_{48}OP_4S_4Se_4U$
fw (g/mol)	1165.04	1420.14	1488.90	1494.89
cryst habit, color	blocks, colorless	blocks, colorless	blocks, yellow	block, yellow-brown
temp (K)	173(2)	173(2)	173(2)	173(2)
space group	$P2_1/n$	$I4_1/a$	$P\bar{1}$	$P\bar{1}$
cryst syst	monoclinic	tetragonal	triclinic	triclinic
volume ($Å^3$)	4403.2(7)	3978.30(16)	2770.7(5)	2728.9(6)
a (Å)	16.4771(14)	19.1065(4)	11.0735(12)	11.0436(15)
b (Å)	15.8152(14)	19.1065(4)	13.4793(15)	13.4223(18)
c (Å)	18.3267(16)	10.8977(3)	18.856(2)	18.694(3)
α (deg)	90.00	90	94.9080(10)	94.9000(10)
β (deg)	112.7790(10)	90	94.7250(10)	95.022(2)
γ (deg)	90.00	90	97.0610(10)	96.663(2)
Z	4	4	2	2
calcd density (Mg/m^3)	1.757	2.371	1.785	1.819
abs coeff (mm^{-1})	3.956	22.248	5.621	5.949
final R indices [$I > 2\sigma(I)$]	$R_w = 0.1152$	$R_w = 0.0653$	$R_w = 0.1071$	$R_w = 0.1248$
	$R_{all} = 0.0616$	$R_{all} = 0.0249$	$R_{all} = 0.0358$	$R_{all} = 0.0548$

The Neu and Gaunt groups have worked with imidodiphosphinochalcogenide, $[N(EPR_2)_2]^-$, E = S, Se, Te, ligands to synthesize rare examples of homoleptic U(III) compounds with U–S,[21,22] U–Se, and U–Te bonds.[23] Additionally, Gaunt and co-workers recently reported the first diselenophosphinate actinide complexes with U(IV), Np(IV), and Pu(III).[24] These compounds were shown to have some covalent bonding character in the 5f elements with more ionic bonding in lanthanide–element bonds.[25,26]

Given our objective and the knowledge that no f element dithio-[27] or diselenophosphonate[28] complexes have been reported, we describe the synthesis of the first dithio- and diselenophosphonate complexes with an actinide. Each complex has been characterized using ¹H and ³¹P NMR and IR spectroscopy, and the bonding has been probed using density functional theory (DFT) calculations. Structural determination by X-ray crystallography is reported for a thorium dithiophosphonate, a thorium diselenophosphonate, and both thorium and uranium thioselenophosphinate complexes.

■ EXPERIMENTAL SECTION

General Considerations. The syntheses and manipulations described below were conducted using standard Schlenk and glovebox techniques. All reactions were conducted in a Vacuum Atmospheres inert atmosphere (Ar or N₂) glovebox. Lawessons' reagent, Woollins'

reagent, sodium methoxide, and potassium *tert*-butoxide (Aldrich) were used as received. ThCl$_4$(DME)$_2$,[29] [Se$_2$P(C$_6$H$_5$)(OMe)]$^-$,[30] UI$_4$(1,4-dioxane)$_2$,[31] Na[SSePPh$_2$]$^-$,[32] and [S$_2$P(4-MeOC$_6$H$_4$)(OMe)]$^-$ were synthesized as previously described.[33] Benzene-d_6, THF-d_8, and acetonitrile-d_3 (Cambridge Isotope Laboratories) were dried over molecular sieves and degassed with three freeze–evacuate–thaw cycles. All ^{1}H, ^{13}C, ^{31}P, and ^{77}Se NMR data were obtained on a 250 MHz ARX, 300 MHz DRX, or 500 MHz DRX Bruker spectrometer. ^{1}H NMR shifts given were referenced internally to the residual solvent peaks at δ 7.16 ppm (C$_6$D$_5$H), 1.94 ppm (CD$_2$HCN), and 3.58 ppm (C$_4$D$_7$HO). ^{13}C NMR shifts were referenced internally to the residual peaks at δ 128.0 ppm (C$_6$D$_6$), 118.3 ppm (CD$_3$CN), and 67.2 ppm (C$_4$D$_8$O). ^{31}P NMR spectra were externally referenced to 0.00 ppm with 5% H$_3$PO$_4$ in D$_2$O. ^{77}Se NMR spectra were externally referenced to 460.00 ppm with PhSeSePh in C$_6$D$_6$. Infrared spectra were recorded as KBr pellets on a Perkin-Elmer Spectrum One FT-IR spectrometer. UV–vis spectra were recorded on a Varian CARY 100 Bio spectrophotometer. Elemental analyses were performed by Atlantic Microlab, Inc. (Norcross, GA, USA).

Crystallographic Data Collection and Structure Determination. The selected single crystal was mounted on nylon cryoloops using viscous hydrocarbon oil. X-ray data collection was performed at 173(2) K. The X-ray data were collected on a Bruker CCD diffractometer with monochromated Mo-Kα radiation (λ = 0.71073 Å) or Cu-Kα (λ = 1.54178 Å). The data collection and processing utilized Bruker Apex2 suite of programs.[34] The structures were solved using direct methods and refined by full-matrix least-squares methods on F2 using Bruker SHELX-97 program.[35] All non-hydrogen atoms were refined with anisotropic displacement parameters. All hydrogen atoms were added on idealized positions and not allowed to vary. Thermal ellipsoid plots were prepared by using X-seed[36] with 50% of probability displacements for non-hydrogen atoms. Crystal data and detail for data collection for complexes **2**, **5**, **7**, and **8** are provided in Table 1, and significant bond distances and angles are gathered in Tables 4 and 5.

Computational Details. Hybrid DFT calculations were carried out using the PBE0 functional[37] in the Gaussian09 Rev. C.01 suite of software.[38] Spin-unrestricted calculations were performed on all open-shell molecules; the formal f^2 configuration for U(IV) was applied. The "ultrafine" integration grid was employed for all calculations, together with the default geometry convergence criteria and with the SCF convergence set to 10^{-6}. For the geometry optimizations, the small core Stuttgart–Bonn variety relativistic pseudopotentials (RPPs) were employed for the f elements, together with the associated segmented valence basis sets (without g functions).[39,40] For Se, the analogous RPP was employed, with valence functions contracted at the TZP level.[41] Dunning's cc-pVTZ basis set was used for S, and the cc-pVDZ basis sets were employed for all other elements. Single-point calculations were performed at the optimized geometries using the segmented all-electron relativistic basis sets with polarization functions (SARCP) for the f elements,[42,43] Dunning's cc-pVTZ basis sets for S and Se, and cc-pVDZ for all other elements.[44] Point charge nuclei were used, as recommended for the SARCP basis set, rather than the default Gaussian form. Relativistic effects were included by using the spin–orbit-free Douglas–Kroll–Hess Hamiltonian. The resulting formatted checkpoint files were then used as input to the AIMAll package version 13.01.27,[45] for QTAIM analysis. Cartesian atomic coordinates for all computationally studied complexes are collected in the Supporting Information.

K[S$_2$P(4-MeOC$_6$H$_4$)(O^{t}Bu)] (1). Following a modified procedure of Li[(4-MeOC$_6$H$_4$)(^{t}BuO)PS$_2$],[46] a 125 mL Schlenk flask was charged with ^{t}BuOK (1.14 g, 10.16 mmol) and dissolved in 30 mL of THF. Lawessons' reagent (2.0 g, 4.944 mmol) was added to the solution, and the mixture was stirred for 18 h at room temperature. The reaction mixture was filtered over a bed of Celite, and the solvent removed *in vacuo*, resulting in a white solid. The white solid was washed with hexanes and diethyl ether (30 mL) and dried to yield a white powder (2.95 g, 95%). ^{1}H NMR (C$_4$D$_8$O, 25 °C): δ 8.10 (dd, 2H, $^3J_{P-H}$ = 13.5 Hz, $^3J_{H-H}$ = 8.5 Hz, *ortho*), 6.74 (dd, 2H, $^3J_{H-H}$ = 8.5 Hz, $^4J_{P-H}$ = 2.5 Hz, *meta*), 3.75 (s, 3H, O*Me*), 1.47 (s, 9H, O^{t}Bu).

^{13}C{^{1}H} NMR (C$_4$D$_8$O, 25 °C): δ 160.96 (d, $^4J_{P-C}$ = 2.5 Hz), 141.37 (d, $^1J_{P-C}$ = 117.0 Hz), 132.37 (d, $^2J_{P-C}$ = 13.8 Hz), 112.37 (d, $^3J_{P-C}$ = 13.8 Hz), 80.39 (d, $^2J_{P-C}$ = 11.3 Hz), 55.30, 31.10. ^{31}P{^{1}H} NMR (C$_4$D$_8$O, 25 °C): δ 95.32. IR (cm^{-1}): 2979 (m), 1594 (s), 1571 (w), 1497 (s), 1384 (s), 1291 (m), 1247 (s), 1178 (m), 1104 (s), 1012 (w), 938 (s), 903 (s), 836 (w), 811 (w), 799 (w), 724 (w), 683 (s), 646 (m), 629 (w), 566 (w), 522 (s). Anal. Calcd for C$_{11}$H$_{16}$KO$_2$PS$_2$: C, 42.02; H, 5.13. Found: C, 41.76; H, 5.27.

Th[S$_2$P(4-MeOC$_6$H$_4$)(OMe)]$_4$ (2). ThCl$_4$(DME)$_2$ (200 mg, 0.361 mmol) was added to a stirred solution of Na[S$_2$P(4-MeOC$_6$H$_4$)(OMe)] (370 mg, 1.44 mmol) in 15 mL of THF and stirred for 18 h. The THF was removed under vacuum, the solid was extracted with toluene and filtered, and the solvent was removed *in vacuo* to yield a white solid (299 mg, 71%). Colorless crystals were grown at room temperature from a concentrated toluene solution. ^{1}H NMR (C$_6$D$_6$, 25 °C): δ 8.09 (dd, 8H, $^3J_{P-H}$ = 14.0 Hz, $^3J_{H-H}$ = 8.0 Hz, *ortho*), 6.57 (dd, 8H, $^3J_{H-H}$ = 8.0 Hz, $^4J_{P-H}$ = 3.0 Hz, *meta*), 3.64 (d, 12H, $^3J_{P-H}$ = 22.0 Hz, O*Me*), 3.12 (s, 12H, O*Me*). ^{13}C{^{1}H} NMR (C$_6$D$_6$, 25 °C): δ 162.85, 132.38 (d, $^2J_{P-C}$ = 15.0 Hz), 129.71 (d, $^1J_{P-C}$ = 128.0 Hz), 113.77 (d, $^3J_{P-C}$ = 16.2 Hz), 54.70, 52.22 (d, $^2J_{P-C}$ = 6.3 Hz). ^{31}P{^{1}H} NMR (C$_6$D$_6$, 25 °C): δ 93.45. IR (cm^{-1}): 2941 (m), 1593 (s), 1570 (m), 1500 (s), 1457 (m), 1384 (m), 1296 (m), 1257 (s), 1180 (s), 1113 (s), 1018 (s), 832 (m), 803 (m), 778 (s), 723 (w), 717 (w), 661 (s), 644 (m), 626 (m), 620 (m), 542 (s). Anal. Calcd for C$_{32}$H$_{40}$O$_8$P$_4$S$_8$Th: C, 32.99; H, 3.46. Found: C, 32.96; H, 3.48.

Th[S$_2$P(4-MeOC$_6$H$_4$)(O^{t}Bu)]$_4$ (3). Following the same procedure as **2** using ThCl$_4$(DME)$_2$ (166 mg, 0.300 mmol) and K[S$_2$P(4-OMeC$_6$H$_4$)(O^{t}Bu)] (377 mg, 1.20 mmol) yielded a white solid (264 mg, 66%). ^{1}H NMR (C$_6$D$_6$, 25 °C): δ 8.12 (dd, 8H, $^3J_{P-H}$ = 14.0 Hz, $^3J_{H-H}$ = 8.0 Hz, *ortho*), 6.64 (d, 8H, $^3J_{H-H}$ = 8.0 Hz, *meta*), 3.22 (s, 12H, O*Me*), 1.44 (s, 36H, ^{t}Bu). ^{13}C{^{1}H} NMR (C$_6$D$_6$, 25 °C): δ 162.29, 133.47 (d, $^1J_{P-C}$ = 129.0 Hz), 132.42 (d, $^2J_{P-C}$ = 13.8 Hz), 113.47 (d, $^3J_{P-C}$ = 16.3 Hz), 86.57 (d, $^2J_{P-C}$ = 11.3 Hz), 54.89, 31.11. ^{31}P{^{1}H} NMR (C$_6$D$_6$, 25 °C): δ 78.85. IR (cm^{-1}): 2939 (m), 1595 (m), 1590 (s), 1369 (m), 1255 (s), 1179 (s), 1111 (s), 1020 (m), 977 (m), 916 (m), 831 (m), 801 (m), 719 (m), 677 (m), 654 (m), 625 (m), 552 (w), 536 (m). Anal. Calcd for C$_{44}$H$_{64}$O$_8$P$_4$S$_8$Th: C, 39.63; H, 4.84. Found: C, 39.57; H, 4.73.

U[S$_2$P(4-MeOC$_6$H$_4$)(OMe)]$_4$ (4). UI$_4$(1,4-dioxane)$_2$ (315 mg, 0.342 mmol) was added to a stirred solution of Na[S$_2$P(4-MeOC$_6$H$_4$)(OMe)] (350 mg, 1.37 mmol) in 15 mL of THF, and the solution underwent an immediate color change from orange to dark green. The mixture was stirred at room temperature for 8 h, the THF was removed under vacuum, and the solid was extracted with acetonitrile, filtered, and concentrated to yield a dark green solid (395 mg, 99%). ^{1}H NMR (CD$_3$CN, 25 °C): δ 11.19 (s, 8H, Ar*H*, $\nu_{1/2}$ = 45.1 Hz), 9.31 (s, 12H, O*Me*, $\nu_{1/2}$ = 45.1 Hz), 8.70 (s, 8H, Ar*H*, $\nu_{1/2}$ = 21.0 Hz), 4.86 (s, 12H, O*Me*, $\nu_{1/2}$ = 4.3 Hz). ^{31}P{^{1}H} NMR (CD$_3$CN, 25 °C): δ −680.90. IR (cm^{-1}): 2934 (m), 1596 (s), 1502 (s), 1404 (s), 1386 (s), 1258 (m), 1180 (m), 1113 (m), 1019 (m), 836 (m), 667 (s), 646 (m), 631 (m), 546 (s). UV–vis (2.3 × 10^{-3} M, CH$_3$CN): 724 nm (ε = 31 L mol^{-1} cm^{-1}), 707 nm (ε = 61 L mol^{-1} cm^{-1}), 602 nm (ε = 17 L mol^{-1} cm^{-1}), 525 nm (ε = 22 L mol^{-1} cm^{-1}). Despite multiple attempts an acceptable elemental analysis could not be obtained.

Th[Se$_2$P(C$_6$H$_5$)(OMe)]$_4$ (5). ThCl$_4$(DME)$_2$ (130 mg, 0.234 mmol) was added to a stirred solution of Na[Se$_2$P(C$_6$H$_5$)(OMe)] (300 mg, 0.936 mmol) in 15 mL of THF and allowed to react for 18 h. The THF was removed under vacuum, the solid was extracted with toluene and filtered, and the solvent was removed *in vacuo* to yield a tan precipitate (219 mg, 66%). ^{1}H NMR (C$_6$D$_6$, 25 °C): δ 8.14–8.10 (m, 8H, Ar*H*), 7.02–6.95 (m, 12H, Ar*H*), 3.57 (d, 12H, $^3J_{P-H}$ = 16.0 Hz, O*Me*). ^{13}C{^{1}H} NMR (C$_6$D$_6$, 25 °C): δ 138.57, 132.03, 130.67 (d, $^2J_{P-C}$ = 12.5 Hz), 130.34, 53.46. ^{31}P{^{1}H} NMR (C$_6$D$_6$, 25 °C): δ 68.43 (s + d satellites, $^1J_{Se-P}$ = 580.0 Hz). ^{77}Se{^{1}H} NMR (C$_6$D$_6$, 25 °C): δ 221.71 (d, $^1J_{P-Se}$ = 580.0 Hz). IR (cm^{-1}): 2934 (m), 1437 (s), 1384 (s), 1181 (m), 1106 (s), 1018 (s), 997 (s), 836 (w), 775 (m), 743 (m), 712, (m), 687 (m), 668 (w), 549 (m), 530 (w), 507 (s). Anal. Calcd for C$_{28}$H$_{32}$O$_4$P$_4$Se$_8$Th: C, 23.68; H, 2.27. Found: C, 23.62; H, 2.28.

U[Se$_2$P(C$_6$H$_5$)(OMe)]$_4$ (6). A 20 mL scintillation vial was charged with Na[Se$_2$P(C$_6$H$_5$)(OMe)] (300 mg, 0.936 mmol), dissolved in 15 mL of THF, and placed in a freeze at −24 °C for 10 min. UI$_4$(1,4-dioxane)$_2$ (216 mg, 0.234 mmol) was added, and the solution underwent an immediate color change from orange to dark red. The mixture was stirred for 2 h, then the reaction mixture was filtered, and the THF was removed *in vacuo*. The solid was extracted with toluene and concentrated to yield a red precipitate (144 mg, 43%). ^{1}H NMR (C$_6$D$_6$, 25 °C): δ 11.52 (s, 12H, O*Me*, $\nu_{1/2}$ = 17.3 Hz), 8.67 (t, $^3J_{H-H}$ = 7.5 Hz, 8H, *meta*, $\nu_{1/2}$ = 6.0 Hz), 8.50 (s, 8H, *ortho*, $\nu_{1/2}$ = 11.0 Hz), 8.42 (t, $^3J_{H-H}$ = 7.5 Hz, 4H, *para*, $\nu_{1/2}$ = 4.0 Hz). ^{31}P{^{1}H} NMR (C$_6$D$_6$, 25 °C): δ −925.10. IR (cm^{-1}): 2933 (m), 1479 (w), 1436 (s), 1384 (m), 1180 (m), 1106 (s), 1018 (s), 835 (w), 773 (s), 743 (s), 713 (s), 686 (s), 544 (s), 528 (w), 507 (s). UV−vis (1.5 × 10^{-3} M, C$_7$H$_8$): 737 nm (ε = 223 L mol^{-1} cm^{-1}), 707 nm (ε = 262 L mol^{-1} cm^{-1}). Anal. Calcd for C$_{28}$H$_{32}$O$_4$P$_4$Se$_8$U: C, 23.58; H, 2.26. Found: C, 23.88; H, 2.27.

Th[SSePPh$_2$]$_4$ (7). ThCl$_4$(DME)$_2$ (99 mg, 0.178 mmol) was added to a stirred solution of Na[SSePPh$_2$] (227 mg, 0.711 mmol) in 15 mL of THF. The mixture was allowed to stir for 12 h to yield a yellow-colored solution. The solution was filtered through Celite and concentrated under vacuum. Colorless crystals grew at room temperature (180 mg, 68%). ^{1}H NMR (C$_6$D$_6$, 25 °C): δ 7.87−7.83 (m, 16H, *ortho*), 6.97 (t, $^3J_{H-H}$ = 7.0 Hz, 8H, *para*), 6.92−6.89 (m, 16H, *meta*). ^{13}C{^{1}H} NMR (C$_6$D$_6$, 25 °C): δ 138.38 (d, $^1J_{P-C}$ = 75.0 Hz, *ipso*), 137.78 (d, $^1J_{P-C}$ = 75.0 Hz, *ipso*), 131.35 (d, $^3J_{P-C}$ = 12.6 Hz, *ortho*), 131.07 (d, $^3J_{P-C}$ = 12.6 Hz, *ortho*), 130.92 (*para*). ^{31}P{^{1}H} NMR (C$_6$D$_6$, 25 °C): δ 33.80 (s + d satellites, $^1J_{Se-P}$ = 528.0 Hz). IR (cm^{-1}): 3050 (m), 1481 (m), 1435 (s), 1384 (m), 1306 (m), 1185 (w), 1098 (s), 1068 (w), 1027 (w), 998 (w), 836 (w), 744 (m), 704 (s), 688 (s), 641 (m), 623 (w), 611 (m), 600 (m), 563 (s), 524 (s), 480 (w). Anal. Calcd for C$_{52}$H$_{48}$OP$_4$S$_4$Se$_4$Th·C$_7$H$_8$: C, 44.82; H, 3.57. Found: C, 44.44; H, 3.40.

U[SSePPh$_2$]$_4$ (8). A 20 mL scintillation vial was charged with UI$_4$(1,4-dioxane)$_2$ (185 mg, 0.2007 mmol). A second scintillation vial was charged with Na[SSePPh$_2$] (256 mg, 0.8027 mmol) and dissolved with 15 mL of CH$_3$CN. The UI$_4$(1,4-dioxane)$_2$ was added to the stirring solution at room temperature and stirred for 2 h to yield a brown-colored solution. The solution was filtered, and the brown solid was dried *in vacuo*. The solid was extracted with THF, filtered, and concentrated. Orange-brown crystals were grown at −24 °C (180 mg, 60%). ^{1}H NMR (C$_6$D$_6$, 25 °C): δ 13.82 (s), 13.29 (s), 12.81 (s), 12.33 (s), 12.27 (s), 11.78 (s), 11.33 (s), 10.88 (t, $^3J_{H-H}$ = 7.5 Hz), 9.39 (t, $^3J_{H-H}$ = 7.5 Hz), 9.24 (t, $^3J_{H-H}$ = 7.5 Hz), 9.11 (t, $^3J_{H-H}$ = 7.5 Hz), 8.99 (t, $^3J_{H-H}$ = 7.5 Hz), 8.93 (t, $^3J_{H-H}$ = 7.5 Hz), 8.85 (t, $^3J_{H-H}$ = 7.5 Hz), 8.81 (t, $^3J_{H-H}$ = 7.5 Hz), 8.76 (t, $^3J_{H-H}$ = 7.5 Hz), 8.70 (t, $^3J_{H-H}$ = 7.5 Hz), 8.62 (t, $^3J_{H-H}$ = 7.5 Hz), 8.58 (t, $^3J_{H-H}$ = 7.5 Hz), 8.53 (t, $^3J_{H-H}$ = 7.5 Hz), 8.45 (t, $^3J_{H-H}$ = 7.5 Hz), 8.36 (t, $^3J_{H-H}$ = 7.5 Hz). ^{31}P{^{1}H} NMR (C$_6$D$_6$, 25 °C): δ −585.62, −591.01, −679.85, −686.71. IR (cm^{-1}): 3052 (m), 1481 (w), 1436 (s), 1384 (s), 1306 (m), 1184 (w), 1158 (w), 1098 (s), 1068 (w), 1027 (w), 998 (w), 836 (w), 744 (m), 704 (s), 688 (s), 638 (w), 611 (w), 597 (w), 566 (s), 524 (s), 479 (w). UV−vis (1.4 × 10^{-3} M, C$_4$H$_8$O): 729 nm (ε = 115 L mol^{-1} cm^{-1}), 710 nm (ε = 192 L mol^{-1} cm^{-1}), 607 nm (ε = 67 L mol^{-1} cm^{-1}). Anal. Calcd for C$_{52}$H$_{48}$OP$_4$S$_4$Se$_4$U·C$_7$H$_8$: C, 44.65; H, 3.56. Found: C, 44.40; H, 3.42.
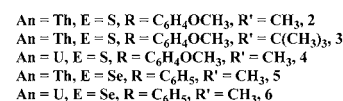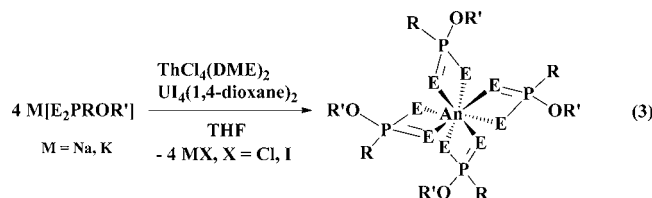
■ RESULTS AND DISCUSSION

Synthesis. The alkali metal dithio- and diselenophosphonates are synthesized by reaction of the corresponding alkali metal alkoxide with Lawesson's, eq 1, or Woollins' reagent, eq 2, respectively. Both sodium methoxide and potassium *tert*-butoxide were used with Lawesson's reagent, but only the methoxide with Woollins' reagent as the corresponding diselenophosphonate actinide complexes was found to be stable. The −O^{t}Bu derivative has not been reported, so we provide analytical and spectroscopic evidence for its synthesis

$$M = Na, R = CH_3$$
$$M = K, R = {}^tBu$$
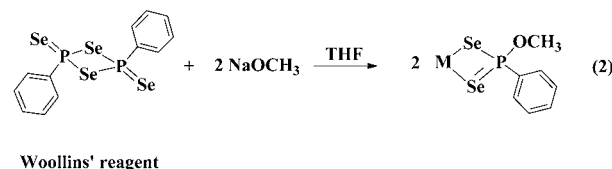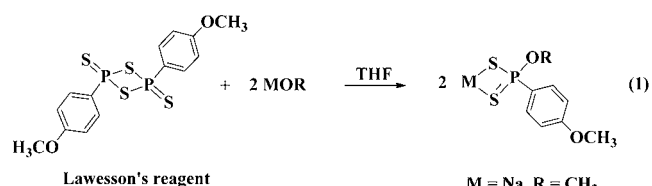
from reaction of Lawesson's reagent with KO^{t}Bu in THF, producing KS$_2$(4-MeOC$_6$H$_4$)(O^{t}Bu) (**1**).

Next, a collection of actinide dichalcogenophosphonates (An[E$_2$PROR′]$_4$, An = Th, U; E = S, Se; R = 4-MeOC$_6$H$_4$, C$_6$H$_5$; R′ = Me, ^{t}Bu) was made from the metathesis reaction between the actinide tetrahalide and alkali metal dithio- or diselenophosphonate, eq 3. Th[S$_2$P(4-MeOC$_6$H$_4$)(OMe)]$_4$ (**2**)

An = Th, E = S, R = C$_6$H$_4$OCH$_3$, R′ = CH$_3$, 2
An = Th, E = S, R = C$_6$H$_4$OCH$_3$, R′ = C(CH$_3$)$_3$, 3
An = U, E = S, R = C$_6$H$_4$OCH$_3$, R′ = CH$_3$, 4
An = Th, E = Se, R = C$_6$H$_5$, R′ = CH$_3$, 5
An = U, E = Se, R = C$_6$H$_5$, R′ = CH$_3$, 6

was isolated by recrystallization from a concentrated solution of toluene at room temperature, giving colorless crystals in 71% yield. Th[S$_2$P(4-MeOC$_6$H$_4$)(O^{t}Bu)]$_4$ (**3**) was synthesized in a similar manner.

To obtain the mixed-chalcogen complexes, we turned to phosphinates, as these can be readily prepared from chlorodiphenylphosphine, elemental sulfur, selenium powder, and sodium hydroxide in a one-pot reaction.[32] The reaction of 1:4 actinide tetrahalide to sodium thioselenophosphinate resulted in the formation of Th[SSePPh$_2$]$_4$ (**7**) and U-[SSePPh$_2$]$_4$ (**8**), eq 4.
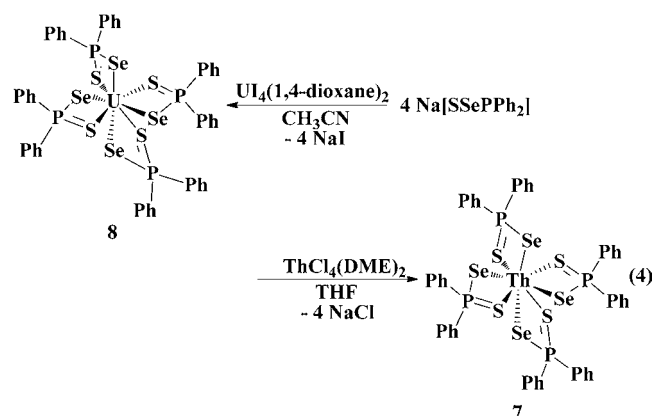
Table 2. ^{31}P NMR Resonances for Complexes 1−8

	1	2	3	4	5	6	7	8
^{31}P resonance (ppm)	95.32	93.45	78.85	−680.90	68.43	−925.10	33.80	−585.62, −591.01, −679.85, −686.71

Table 3. Infrared Spectroscopy Data for Complexes 1−8

bond stretching frequency (cm^{-1})	1	2	3	4	5	6	7	8
ν(C−H)	2979	2941	2939	2934	2934	2933	3050	3052
ν[(P)−O−C]	1178	1180	1179	1180	1181	1180		
ν[P−O−(C)]	1012	1018	1020	1019	1018	1018		
ν(C−O)	1104	1113	1111	1113	1106	1106		
ν(P−S)$_{asym}$	683	661	677	667			688	688
ν(P−S)$_{sym}$	566	542	536	546				
ν(P−Se)$_{asym}$					549	544	524	524
ν(P−Se)$_{sym}$					507	507		

To take advantage of the strained four-membered ring of complexes **2** and **3**, reactions with substrates with the potential to undergo insertion in the metal−chalcogen bond were investigated. However, with the heteroallenes CO_2, CS_2, and PhNCO, no reactions were observed even upon heating.

NMR Spectroscopy. Complexes **2** and **3** display similar NMR spectra with both revealing an AB splitting pattern for the aromatic protons with coupling to phosphorus. The ^{31}P NMR spectrum of **2** showed a chemical shift at 93.45 ppm, while **3** saw a significant shift upfield to 78.85 ppm. We attribute the change in chemical shift to the increased basicity of the −O^{t}Bu versus the −OMe group as observed in the chemical resonances for Na[S$_2$P(4-MeOC$_6$H$_4$)(OMe)] and K[S$_2$P(4-MeOC$_6$H$_4$)(O^{t}Bu)], 107.97 and 95.32 ppm, respectively. The ^{31}P NMR spectrum of complex **3** displayed a single resonance at −680.90 ppm, which can be explained by the paramagnetism of U^{4+}. The ^{31}P spectrum of **5** displayed a singlet at 68 ppm with selenium satellites ($^1J_{Se−P}$ = 580.0 Hz). Due to the paramagnetic nature of **6**, the observed ^{31}P signal occurred at −925 ppm. The ^{77}Se NMR of **5** displayed a doublet at 222 ppm with matching ^{31}P−^{77}Se coupling constant. To our knowledge, this is the first report of a ^{77}Se NMR spectrum when the selenium is bound to the actinide. Previously, a shift of −316 ppm was observed for the thorium selenocyanate complex, Th(NCSe)$_4$[OP(NMe$_2$)$_3$]$_4$.[47]

The ^{13}C NMR spectrum of **7** displayed two inequivalent *ipso*-carbon and *ortho*-carbon atoms, while the resonance signal of the meta-carbon was buried under the solvent peak. The ^{31}P NMR spectrum showed a singlet split by selenium satellites ($^1J_{Se−P}$ = 528.0 Hz) for complex **7**. There is significant decrease in the ^{31}P−^{77}Se coupling constant for **7** (528 Hz) when compared to **5** (580 Hz), suggesting a decrease in the bond order of the P−Se bond. Unfortunately the ^{77}Se NMR for **7** could not be obtained. The ^{1}H NMR spectrum of **8** showed eight different signals in the range 13.82−10.88 ppm in various intensities representing the *ortho*-protons. The matching *meta*- and *para*-protons fell in the range 9.38−8.36 ppm (confirmed using correlation NMR spectroscopy). Initially, **8** was thought to contain a mixture of isomers, but upon heating, there was no coalescence of the resonances into one isomer or any change in intensities of peaks. We believe that each phenyl ring is in its own unique chemical environment, and this explains the splitting pattern observed, but we do not know why this is not seen in **7**. The ^{31}P NMR spectrum of **8** also showed multiple peaks indicating the inequivalency of each phosphorus atom.

Infrared Spectroscopy. Phosphonate and phosphinate complexes have several distinct IR stretching frequencies, which are summarized in Table 3. For example, the dithiophosphonates, **1−4**, have strong bands at 683, 661, 677, and 667 cm^{-1}, respectively, which are attributed to the ν(P−S)$_{asym}$ stretch as well as 566, 542, 536, and 546 cm^{-1}, respectively, for ν(P−S)$_{sym}$. Complexes **5** and **6** contain two strong bands at 549 and 507 cm^{-1} for **5** and 544 and 507 cm^{-1} for **6** corresponding to the ν(P−Se)$_{asym}$ and ν(P−Se)$_{sym}$ stretches, respectively. The phosphonate complexes also contain strong bands around 1180 cm^{-1} for ν[(P)−O−C] and 1020 cm^{-1} for the ν[P−O−(C)]. The thioselenophosphinate complexes, **7** and **8**, showed strong bands only at 688 and 524 cm^{-1}, which correspond to the asymmetric P−S and P−Se stretches, respectively. Other transition metal complexes with dithiophosphonate[48] and diselenophosphonate[30] ligands show similar stretching frequencies.

X-ray Crystallography. The geometry environment the dithiophosphonate ligands in **2**, Figure 2, adopt around the metal center can be described as trigonal dodecahedron with the 16th, 17th, and 18th ligand−metal−ligand bond angles being 81.15(4)°, 80.30(4)°, and 79.11(4)°, respectively, as
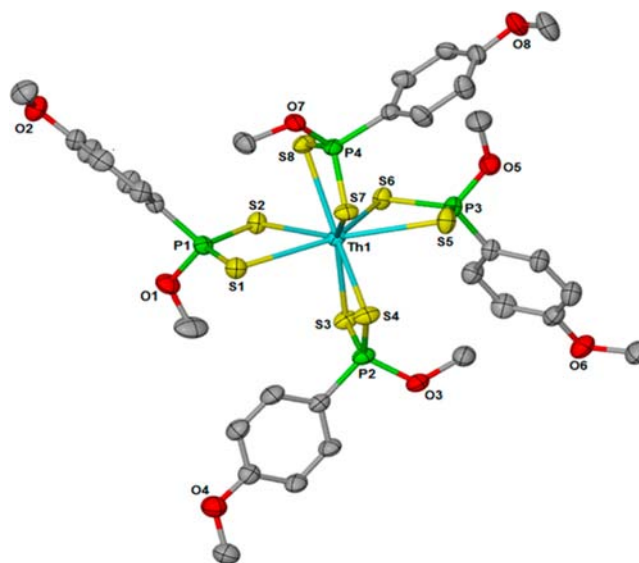

Figure 2. Molecular structure of Th[S$_2$P(4-MeOC$_6$H$_4$)(OMe)]$_4$ (**2**) shown at the 30% probability level. Hydrogen atoms have been omitted for clarity.

Table 4. Selected Bond Distances (Å) and Angles (deg) for Th[S$_2$P(4-MeOC$_6$H$_4$)(OMe)]$_4$ (2), Th[S$_2$P(4-MeOC$_6$H$_4$)(OMe)]$_4$ (Calculated, 2a), U[S$_2$P(4-MeOC$_6$H$_4$)(OMe)]$_4$ (Calculated, 4a), Th[Se$_2$P(C$_6$H$_5$)(OMe)]$_4$, (5), Th[Se$_2$P(4-MeOC$_6$H$_4$)(OMe)]$_4$ (Calculated, 5a), and U[Se$_2$P(4-MeOC$_6$H$_4$)(OMe)]$_4$ (Calculated, 6a)

	2, E = S	2a, E = S	4a, E = S	5, E = Se	5a, E = Se	6a, E = Se
M−E1	2.9222(12)	2.9272	2.8847	3.0472(1)	3.0740	3.0152
M−E2	2.8615(14)	2.8917	2.8114	3.0077(1)	3.0209	2.9700
M−E3	2.8849(13)	2.8895	2.8086	3.0472(1)	3.0757	3.0192
M−E4	2.8961(13)	2.9275	2.8852	3.0077(1)	3.0224	2.9699
M−E5	2.8646(13)	2.8900	2.8110	3.0472(1)	3.0747	3.0312
M−E6	2.9167(13)	2.9250	2.8846	3.0077(1)	3.0227	2.9518
M−E7	2.9258(12)	2.9263	2.8816	3.0472(1)	3.0756	3.0484
M−E8	2.8838(12)	2.8919	2.8089	3.0077(1)	3.0244	2.9585
E1−M1−E2	69.56(4)	69.48	70.26	71.40(1)	71.53	72.26
E3−M1−E4	69.15(4)	69.45	70.26	74.46(1)	71.47	72.21
E5−M1−E6	68.96(4)	69.45	70.18	71.40(1)	71.46	72.13
E7−M1−E8	68.87(3)	69.41	70.17	74.46(1)	71.41	71.80

described by Haigh.[49] Each of the sulfur atoms is bonded to the thorium, giving a coordination number of eight. One [S$_2$P(4-MeOC$_6$H$_4$)(OMe)]$^-$ ligand is coplanar with one other and almost orthogonal to the other two. Another distinct feature of **2** is that each ligand pair is composed of one short and one long Th−S bond. The Th−S bond distances and S−Th−S angles are shown in Table 4 with the average being 2.8944(13) Å and 69.13(4)°. This value compares well to the average Th−S bond distance of 2.911(4) Å and S−Th−S angles of 68.7(1)° in Th[S$_2$PPh$_2$]$_4$.[12] The agreement between the experimental geometry of **2** and that calculated using DFT (**2a**) is excellent. The average calculated An−S bond distance decreases from 2.9086 Å for **2a** to 2.8470 Å for **3a**, very much in keeping with the decrease in the eight-coordinate ionic radius from Th^{4+} to U^{4+} (1.05 vs 1.00 Å).[50]

Complex **5** is the first homoleptic thorium complex with selenium atoms, and only two other complexes exist with Th−Se linkages, Figure 3. The average Th−Se bond distance of 3.0274(1) Å in **5** is the longest since (1,2,4-^{t}Bu$_3$C$_5$H$_2$)$_2$Th-
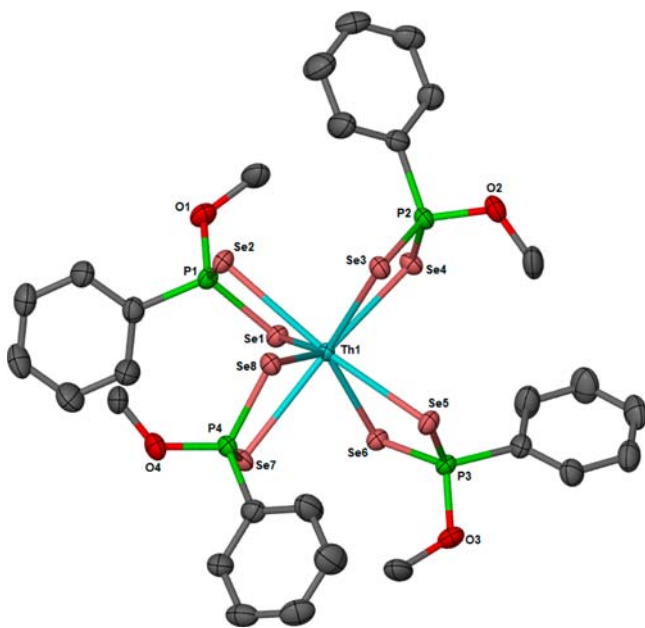
(SePh)$_2$ and (1,2,4-^{t}Bu$_3$C$_5$H$_2$)Th(SePh)$_3$(bipy) reported average Th−Se distances of 2.938(8)[51] and 2.877 Å,[52] respectively.

Upon refinement for both **7** and **8**, it was determined the S and Se atoms were occupying the same site. To alleviate this problem, the occupancy was split 50/50 between each sulfur and selenium atom of the [SSeP]$^-$ bidentate ligand. As a result, no meaningful data could be determined as to the actinide preference of sulfur or selenium, but a general connectivity model was obtained. Each of the four [SSeP]$^-$ ligands coordinates to the metal center through the sulfur and selenium atoms, giving rise to a coordination number of eight, Figure 4. The geometry of **7** and **8** can be described as dodecahedron following Haigh's criteria with the 16th, 17th, and 18th ligand−metal−ligand angles being 78.59(5)°, 78.12(5)°, and 77.81(5)°; 77.79(4)°, 77.57(4)°, and 77.31(4)°, respectively. Selected bond angles and distance are shown in Table 5. The average bond distances for complexes **7** and **8** are 2.9756(18) and 2.9047(12) Å, respectively. As for **2a** and **3a**, we attribute the decrease in bond length observed in **8** to the decrease in ionic radius of the U^{4+} cation versus Th^{4+}.[50] The difference in average bond lengths between **7** and **8** is 0.071 Å, suggesting no major differences in An−E bonding between Th and U. The average bite angles for **7** and **8** are 71.97(5)° and 72.42(5)°, respectively. Like complex **2** the trend of one short and one long An−E bond for each EPE moiety carries over in **7** and **8**, illustrated clearly in the calculated structures of **7a** and **8a**; the average An−S are 2.9062 and 2.8483 Å, while for An−Se the values are 3.0493 and 2.9983 Å for Th and U, respectively.

Density Functional Theory Calculations. To gain insight into the actinide−sulfur and −selenium bonds, we turned to density functional theory. We, as well as others, have previously examined Mulliken spin densities to determine the extent to which electron density is distributed between the metal and ligands since the spin density is independent of the functional and basis set used in the calculation.[53−56] Another method that has gained recent traction in describing f element bonding[57,58] is the quantum theory of atoms in molecules (QTAIM)[59] and, in particular, the properties of metal−ligand bond critical points (BCPs). Data for the electron and energy densities at the An−E BCPs in 10 calculated complexes are collected in Table 6, as are the An−E delocalization indices (DIs). The absolute values of ρ and H are small, suggesting only a small amount of covalent interaction between the actinide and ligand. For a given metal, the BCP parameters are all slightly smaller for the An−Se
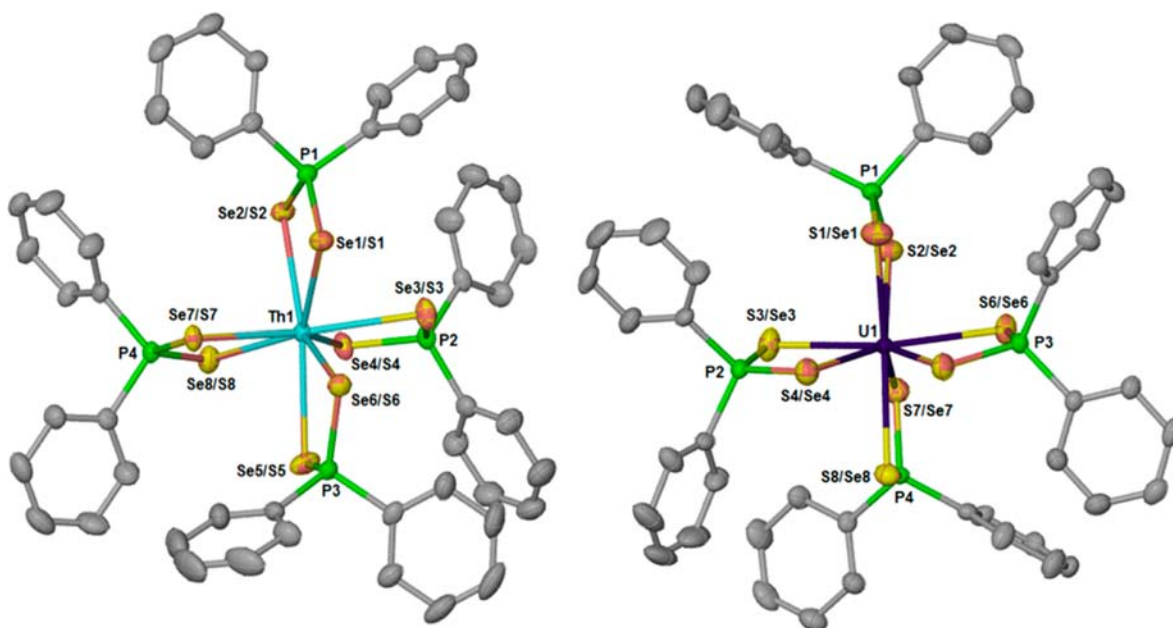

Figure 3. Molecular structure of Th[Se$_2$P(C$_6$H$_5$)(OMe)]$_4$ (**5**) shown at the 50% probability level. Hydrogen atoms have been omitted for clarity.

Figure 4. Molecular structure of Th[SSePPh₂]₄ (**7**) and U[SSePPh₂]₄ (**8**) shown at the 30% probability level. Hydrogen atoms have been omitted for clarity.

Table 5. Selected Bond Distances (Å) and Angles (deg) for Th[SSePPh₂]₄ (7) and U[SSePPh₂]₄ (8)

	7	8
M−S1/Se1	3.0047(17)	2.9574(12)
M−S2/Se2	2.9573(17)	2.8491(13)
M−S3/Se3	2.9344(19)	2.9354(13)
M−S4/Se4	3.0159(17)	2.8611(12)
M−S5/Se5	2.9342(19)	2.9406(13)
M−S6/Se6	3.0008(18)	2.8774(11)
M−S7/Se7	2.9731(16)	2.9142(13)
M−S8/Se8	2.9848(19)	2.9021(11)
S1/Se1−M1−S2/Se2	72.33(5)	72.37(4)
S3/Se3−M1−S4/Se4	71.86(5)	72.32(4)
S5/Se5−M1−S6/Se6	71.94(5)	72.80(3)
S7/Se7−M1−S8/Se8	71.75(5)	72.20(3)

bonds than the An−S. Rather than conclude that An−Se bonding is less covalent than An−S, we attribute this to the

significantly (ca. 0.15 Å) longer An−Se bonds than the An−S. ρ and H typically show a strong dependence on bond length, and we have previously found BCP metrics for An−S and An−Se systems in which the metal−chalcogen distances are fixed to be equal to show significantly higher values for An−Se. For example, we recently reported ρ at the Th−Se BCPs in Th(Se₂PMe₂)₄ to be 0.043 e/bohr³.[24] This increases to 0.052 e/bohr³ when the Th−Se bond distances are set to the Th−S distances obtained from geometry optimization of Th-(S₂PMe₂)₄. ρ(BCP) for Th−S at the optimized Th(S₂PMe₂)₄ distance is only 0.047 e/bohr³. Thus a reduction in the Th−Se distance of ca. 0.15 Å generates a ca. 0.01 e/bohr³ increase in ρ(BCP), and ρ(BCP) for Th−Se is 0.005 e/bohr³ larger than Th−S for identical Th−chalcogen distances. Table 6 reveals ρ and H to be all absolutely larger in U complexes versus their Th counterparts, by an amount similar to the difference between S and Se systems for a given metal. Here, however, the differences in U−E versus Th−E bond lengths are much smaller (ca. 0.05

Table 6. Characteristics of the Actinide−Ligand Bond Critical Points and An−E Delocalization Indices in Thorium and Uranium Dithiophosphonates, Dithiophosphinates, Diselenophosphonates, Diselenophosphinates, and Thioselenophosphinates[a]

	bond type	ρ	H	DI
Th[S₂P(4-OMeC₆H₄)(OCH₃)]₄, **2a**	Th−S	0.047, 0.042	−0.008, −0.008	0.409, 0.375
Th[S₂PPh₂]₄	Th−S	0.047, 0.044	−0.008, −0.007	0.409, 0.374
Th[Se₂P(4-OMeC₆H₄)(OCH₃)]₄	Th−Se	0.042, 0.039	−0.007, −0.007	0.416, 0.375
Th[Se₂PPh₂]₄	Th−Se	0.042, 0.039	−0.008, −0.007	0.419, 0.376
Th[SSePPh₂]₄, **7a**	Th−S	0.047, 0.042	−0.009, −0.007	0.418, 0.381
	Th−Se	0.044, 0.039	−0.007, −0.006	0.412, 0.367
U[S₂P(4-OMeC₆H₄)(OCH₃)]₄, **4a**	U−S	0.053, 0.045	−0.010, −0.008	0.481, 0.407
U[S₂PPh₂]₄	U−S	0.052, 0.045	−0.010, −0.008	0.487, 0.415
U[Se₂P(4-OMeC₆H₄)(OCH₃)]₄	U−Se	0.047, 0.042	−0.009, −0.007	0.507, 0.453
U[Se₂PPh₂]₄	U−Se	0.049, 0.040	−0.009, −0.007	0.555, 0.444
U[SSePPh₂]₄, **8a**	U−S	0.054, 0.046	−0.011, −0.008	0.530, 0.453
	U−Se	0.047, 0.040	−0.009, −0.006	0.523, 0.428

[a]ρ and H in atomic units. Each entry in each data pair is averaged over four An−E bonds.

10629

dx.doi.org/10.1021/ic401642a | *Inorg. Chem.* 2013, 52, 10623−10631

Å), and we conclude, as we have done on previous occasions,[24,57,58] that U−E is more covalent than Th−E.

The DI data also support enhanced covalency in U−E versus Th−E (the DI, or bond index, is a measure of the average number of electrons shared between actinide and the coordinated ligand; large DIs imply more covalent character) and, in 8 of the 10 complexes studied, suggest the An−Se bond is more covalent than the An−S. The exceptions are **7a** and **8a**, which both feature slightly smaller An−Se DIs than An−S. The origin of this behavior is unclear. Our conclusion of greater covalency in actinide−selenium bonds is further supported by comparing the Mulliken spin densities for complexes **4a** and U[Se$_2$P(4-MeOC$_6$H$_4$)(OMe)]$_4$: 2.149 and 2.179, respectively, as well as 2.137 and 2.246 for U[S$_2$PPh$_2$]$_4$ and U[Se$_2$PPh$_2$]$_4$, respectively. The increased deviation from 2.000 indicates more covalent bonding character.

CONCLUSION

In summary, we have synthesized the first actinide dithio- and diselenophosphonates, as well as thioselenophosphinates, and characterized them through elemental analysis and ^{1}H and ^{31}P NMR spectroscopy, as well as using ^{13}C and ^{77}Se NMR spectroscopy with Th[Se$_2$P(C$_6$H$_5$)(OCH$_3$)]$_4$. This is the first time ^{77}Se NMR spectroscopy has been implemented with a compound containing a direct thorium−selenium bond. Th[S$_2$P(4-MeOC$_6$H$_4$)(OMe)]$_4$, Th[Se$_2$(C$_6$H$_5$)(OMe)]$_4$, and An[SSePPh$_2$]$_4$, An = Th, U, were also structurally characterized. Quantum chemical calculations comparing dithio- and diselenophosphonate and phosphinate thorium and uranium complexes have indicated that the actinide−selenium bond has increased covalent character in comparison with the actinide−sulfur. Further studies aimed at verifying our DFT results using X-ray absorption spectroscopy measurements are under way.

ASSOCIATED CONTENT

Ⓢ Supporting Information

Crystallographic details for **2**, **5**, **7**, and **8**, as well as computed geometries, are available free of charge via the Internet at http://pubs.acs.org.

AUTHOR INFORMATION

Corresponding Authors
*E-mail: n.kaltsoyannis@ucl.ac.uk.
*E-mail: walenskyj@missouri.edu

Notes
The authors declare no competing financial interest.

ACKNOWLEDGMENTS

REFERENCES

(1) Choppin, G. R. *J. Less-Common Met.* **1983**, *93*, 323−330.

(2) Diamond, R. M.; Street, K.; Seaborg, G. T. *J. Am. Chem. Soc.* **1954**, *76*, 1461−1469.

(3) Jensen, M. P.; Bond, A. H. *J. Am. Chem. Soc.* **2002**, *124*, 9870−9877.

(4) Klaehn, J. R.; Peterman, D. R.; Harrup, M. K.; Tillotson, R. D.; Luther, T. A.; Law, J. D.; Daniels, L. M. *Inorg. Chim. Acta* **2008**, *361*, 2522−2532.

(5) Tian, G.; Zhu, Y.; Xu, J.; Hu, T.; Xie, Y. *J. Alloys Compd.* **2002**, *334*, 86−91.

(6) Guoxin, T.; Yongjun, Z.; Jingming, X.; Ping, Z.; Tiandou, H.; Yaning, X.; Jing, Z. *Inorg. Chem.* **2003**, *42*, 735−741.

(7) Jones, R. G.; Karmas, G.; Martin, G. A.; Gilman, H. *J. Am. Chem. Soc.* **1956**, *78*, 4285−4286.

(8) Bagnall, K. W.; Holah, D. G. *Nature* **1967**, *215*, 623.

(9) Bagnall, K. W.; Brown, D.; Holah, D. G. *J. Chem. Soc. A* **1968**, 1149−1153.

(10) Brown, D.; Holah, D. G.; Rickard, C. E. F. *J. Chem. Soc. A* **1970**, 423−425.

(11) Brown, D.; Holah, D. G.; Rickard, C. E. F. *J. Chem. Soc. A* **1970**, 786−790.

(12) Pinkerton, A. A.; Storey, A. E.; Zellweger, J.-M. *J. Chem. Soc., Dalton Trans.* **1981**, 1475−1480.

(13) Tatsumi, K.; Matsubara, I.; Inoue, Y.; Nakamura, A.; Cramer, R. E.; Tagoshi, G. J.; Golen, J. A.; Gilje, J. W. *Inorg. Chem.* **1990**, *29*, 4928−4938.

(14) Leverd, P. C.; Lance, M.; Nierlich, M.; Vigner, J.; Ephritikhine, M. *J. Chem. Soc. A* **1993**, 2251−2254.

(15) Leverd, P. C.; Lance, M.; Nierlich, M.; Vigner, J.; Ephritikhine, M. *J. Chem. Soc. A* **1994**, 3563−3567.

(16) Roger, M.; Arliguie, T.; Thuéry, P.; Fourmigué, M.; Ephritikhine, M. *Inorg. Chem.* **2005**, *44*, 594−600.

(17) Meskaldji, S.; Belkhiri, L.; Arliguie, T.; Fourmigué, M.; Ephritikhine, M.; Boucekkine, A. *Inorg. Chem.* **2010**, *49*, 3192−3200.

(18) Roger, M.; Barros, N.; Arliguie, T.; Thuéry, P.; Maron, L.; Ephritikhine, M. *J. Am. Chem. Soc.* **2006**, *128*, 8790−8802.

(19) Arliguie, T.; Thuéry, P.; Floch, P. L.; Mézailles, N.; Ephritikhine, M. *Polyhedron* **2009**, *28*, 1578−1582.

(20) Gaunt, A. J.; Scott, B. L.; Neu, M. P. *Inorg. Chem.* **2006**, *45*, 7401−7407.

(21) Gaunt, A. J.; Scott, B. L.; Neu, M. P. *Chem. Commun.* **2005**, 3215−3217.

(22) Gaunt, A. J.; Reilly, S. D.; Enriquez, A. E.; Scott, B. L.; Ibers, J. A.; Sekar, P.; Ingram, K. I. M.; Kaltsoyannis, N.; Neu, M. P. *Inorg. Chem.* **2007**, *47*, 29−41.

(23) Gaunt, A. J.; Scott, B. L.; Neu, M. P. *Angew. Chem., Int. Ed.* **2006**, *45*, 1638−1641.

(24) Jones, M. B.; Gaunt, A. J.; Gordon, J. C.; Kaltsoyannis, N.; Neu, M. P.; Scott, B. L. *Chem. Sci.* **2013**, *4*, 1189−1203.

(25) Ingram, K. I. M.; Kaltsoyannis, N.; Gaunt, A. J.; Neu, M. P. *J. Alloys Compd.* **2007**, *444−445*, 369−375.

(26) Ingram, K. I. M.; Tassell, M. J.; Gaunt, A. J.; Kaltsoyannis, N. *Inorg. Chem.* **2008**, *47*, 7824−7833.

(27) Van Zyl, W. E.; Woollins, J. D. *Coord. Chem. Rev.* **2013**, *257*, 718−731.

(28) Lobana, T. S.; Wang, J. C.; Liu, C. W. *Coord. Chem. Rev.* **2007**, *251*, 91−110.

(29) Cantat, T.; Scott, B. L.; Kiplinger, J. L. *Chem. Commun.* **2010**, *46*, 919−921.

(30) Gray, I. P.; Slawin, A. M. Z.; Woollins, J. D. *Dalton Trans.* **2005**, 2188−2194.

(31) Monreal, M. J.; Thomson, R. K.; Cantat, T.; Travia, N. E.; Scott, B. L.; Kiplinger, J. L. *Organometallics* **2011**, *30*, 2031−2038.

(32) Artem'ev, A. V.; Gusarova, N. K.; Bagryanskaya, I. Y.; Doronina, E. P.; Verkhoturova, S. I.; Sidorkin, V. F.; Trofimov, B. A. *Eur. J. Inorg. Chem.* **2013**, 415−426.

(33) Aragoni, M. C.; Arca, M.; Demartin, F.; Devillanova, F. A.; Graiff, C.; Isaia, F.; Lippolis, V.; Tiripicchio, A.; Verani, G. *Eur. J. Inorg. Chem.* **2000**, 2239−2244.

(34) Apex II suite, Bruker AXS Ltd.: Madison, WI, 2006.

(35) Sheldrick, G. M. *Acta Cryst.* **2008**, *A64*, 112.

(36) Barbour, L. J. *Supramol. Chem.* **2001**, *1*, 189.

(37) Adamo, C.; Barone, V. *J. Chem. Phys.* **1999**, *110*, 6158−6170.

(38) Frisch, M. J.; Trucks, G. W.; Schlegel, H. B.; Scuseria, G. E.; Robb, M. A.; Cheeseman, J. R.; Scalmani, G.; Barone, V.; Menuuci, B.; Petersson, G. A.; Nakatsuji, H.; Caricato, M.; Li, X.; Hratchian, H. P.; Izmaylov, A. F.; Bloino, J.; Zheng, G.; Sonnenberg, J. L.; Hada, M.; Ehara, M.; Toyota, K.; Fukuda, R.; Hasegawa, J.; Ishida, M.; Nakajima, T.; Honda, Y.; Kitao, O.; Nakai, H.; Vreven, T.; Montgomery, J. A.; Peralta, J. E. J.; Ogliaro, F.; Bearpark, M.; Heyd, J. J.; Brothers, E.; Kudin, K. N.; Staroverov, V. N.; Kobayashi, R.; Normand, J.; Raghavachari, K.; Rendell, A.; Burant, J. C.; Iyengar, S. S.; Tomasi, J.; Cossi, M.; Rega, N.; Millam, J. M.; Klene, M.; Knox, J. E.; Cross, J. B.; Bakken, V.; Adamo, C.; Jaramillo, J.; Gomperts, R.; Stratmann, R. E.; Yazyev, O.; Austin, A. J.; Cammi, R.; Pomelli, C.; Ochterski, J. W.; Martin, R. L.; Morokuma, K.; Zakrzewski, V. G.; Voth, G. A.; Salvador, P.; Dannenberg, J. J.; Dapprich, S.; Daniels, A. D.; Farkas, O.; Foresman, J. B.; Ortiz, J. V.; Cioslowski, J.; Fox, D. J. *Gaussion 09, Revision C.01*; Gaussian, Inc.: Wallingford, CT, 2009.

(39) Cao, X.; Dolg, M. *J. Mol. Struct.: THEOCHEM* **2002**, *581*, 139−147.

(40) Cao, X.; Dolg, M. *J. Mol. Struct.: THEOCHEM* **2004**, *673*, 203−209.

(41) Martin, J. M. L.; Sundermann, A. *J. Chem. Phys.* **2001**, *114*, 3408−3420.

(42) Pantazis, D. A.; Neese, F. *J. Chem. Theory Comput.* **2009**, *5*, 2229−2238.

(43) Pantazis, D. A.; Neese, F. *J. Chem. Theory Comput.* **2011**, *7*, 677−684.

(44) Davison, E. R. *Chem. Phys. Lett.* **1996**, *260*, 514.

(45) Keith, T. A. *AIMAll 13.01.27*; TK Gristmill Software, 2013.

(46) Fild, M.; Krüger, O.; Silaghi-Dumitrescu, I.; Thöne, C.; Weinkauf, A. *Phosphorus, Sulfur, Silicon Relat. Elem.* **2007**, *182*, 2283−2310.

(47) Crawford, M. J.; Karaghiosoff, K.; Mayer, P. Z. *Anorg. Allg. Chem.* **2010**, *636*, 1903−1906.

(48) Gray, I. P.; Slawin, A. M. Z.; Woollins, J. D. *Dalton Trans.* **2004**, 2477−2486.

(49) Haigh, C. W. *Polyhedron* **1995**, *14*, 2871−2878.

(50) Shannon, R. *Acta Crystallogr., Sect. A: Cryst. Phys., Diffr., Theor. Gen. Crystallogr.* **1976**, *32*, 751−767.

(51) Ren, W.; Song, H.; Zi, G.; Walter, M. D. *Dalton Trans.* **2012**, *41*, 5965−5973.

(52) Ren, W.; Zi, G.; Walter, M. D. *Organometallics* **2012**, *31*, 672−679.

(53) Prodan, I. D.; Scuseria, G. E.; Martin, R. L. *Phys. Rev. B* **2007**, *76*, 033101−033104.

(54) Walensky, J. R.; Martin, R. L.; Ziller, J. W.; Evans, W. J. *Inorg. Chem.* **2010**, *49*, 10007−10012.

(55) Fortier, S.; Walensky, J. R.; Wu, G.; Hayton, T. W. *J. Am. Chem. Soc.* **2011**, *133*, 11732−11743.

(56) Mrutu, A.; Lane, A. C.; Drewett, J. M.; Yourstone, S. D.; Barnes, C. L.; Halsey, C. M.; Cooley, J. W.; Walensky, J. R. *Polyhedron* **2013**, *54*, 300−308.

(57) Tassell, M. J.; Kaltsoyannis, N. *Dalton Trans.* **2010**, *39*, 6719−6725.

(58) Kaltsoyannis, N. *Inorg. Chem.* **2013**, *52*, 3407−3413.

(59) Bader, R. F. W. *Atoms in Molecules: A Quantum Theory*; Oxford University Press: Oxford, 1990.